3D Simulation of Solar Cells with Integration of Optical Nanoantennas

Inês Margarida Pinheiro Caetano
ines.p.caetano@tecnico.ulisboa.pt

Instituto Superior Técnico, Universidade de Lisboa, Lisboa, Portugal

***Abstract*—The evolution of nanotechnology has provided a better understanding of light-matter interaction at a subwavelength scale and has led to the development of new devices that can possibly play an important role in future applications, in various fields. Nanoantennas are a prime example of such devices, having gained considerable interest in recent years for their application in the field of photovoltaic technology at visible and infrared wavelengths, due to their ability of capturing and confining energy of free-propagating waves. Some of these devices feature apertures and can benefit from unique optical properties related to the phenomenon of extraordinary optical transmission (EOT) where, due to resonant behavior, light passing through subwavelength apertures in a metal film can be transmitted in greater orders of magnitude than that predicted by classical aperture theory. Nevertheless, the successful implementation of such devices for photovoltaic applications is yet to be achieved. During this study different 2D and 3D models featuring a metallic nanoantenna array with subwavelength holes coupled to a photovoltaic cell, are going to be simulated using COMSOL Multiphysics®. These models present slight variations between them such as the position of the nanoantenna within the structure, the geometry of the holes of the nanoantenna and type of solar cell. The results ultimately demonstrate that the coupling of nanoantennas to solar cells can indeed be advantageous and improve the capture and absorption of solar energy by the cells.**

***Keywords*: apertures; nanoantenna; photovoltaic; solar cells; subwavelength structures.**

I. Introduction

Energy demand has been steadily increasing since the Industrial Revolution and should continue to increase, accompanied by global population growth.

Although renewable energy use is increasing globally, as of 2018 these sources of energy only accounted for less than 20% of the world's primary energy consumption [1]. Fossil fuels such as oil, coal and natural gas still meet much of the world's energy demand. Concerns over climate change and the energy demand of a rapidly growing global population, require an urgent shift towards renewable resources for energy production. Renewables are forecast to become the leading source of primary energy consumption by 2050, with wind and solar representing 70% of total renewables generation [1].

Nowadays, photovoltaic (PV) cells can make a direct conversion of the power associated with solar radiation into DC electric power, at a relatively low cost. In addition, the fact that PV cells are robust structures that require very little maintenance makes them an extremely attractive technology that is rapidly expanding on the global energy market [2]. However, PV solar cells have some limitations. Only a small fraction of the incoming solar radiation can be converted to electricity by semiconductors due to the materials characteristics and electrical properties. Even though many research efforts have been put into place in order to improve efficiency rates of PV solar panels, the optimization of these efficiency rates has yet to be achieved. Most panels present efficiency rates of around 20% or less, usually requiring a mechanical sun-tracking system to optimize conversion. Nanotechnology can be part of the solution to this problem [3].

The field of nanotechnology and optical materials has experienced a rapid advancement which has led to the emergence and development of new systems and devices, like the nanoantenna. With the implementation of this technology, PV solar devices are expected to become more efficient and inexpensive [4]. In this investigation the use of nanotechnology in photovoltaics is going to be studied by simulating 2D and 3D structures of a nanoantenna coupled with a solar cell. The optical response of such structures is going to be discussed and compared. Finally, based on that analysis, the goal is to understand whether the integration of nanoantennas in solar cells can actually bring advantages or additional improvements with regard to the process of solar energy harvesting and, of all models simulated, which one is best suited for this propose.

II. Nanoantennas for Solar Energy Harvesting

Photovoltaic panels are currently the most used technology for converting solar energy into electricity. Although PV technology has improved a lot in recent years, it is still not able to fully utilize the abundance of solar energy reaching the earth in the visible and infrared regions and the reradiated infrared energy [5]. Moreover, as a quantum device, the efficiency of PV is a function of the bandgap and the match of the bandgap to the solar spectrum and, therefore, is also restricted by it [6]. Furthermore, PV materials are typically only operational during daylight hours and require direct solar radiation for optimal efficiency.

Optical antennas are devices that convert propagating optical radiation into localized energy, and vice versa. They can control and manipulate optical radiation at subwavelength scales [7]. Thus, if coupled with PV solar panels, the overall

efficiency of the system is expected to be higher than the current efficiency rate of solar panels. Optical nanoantennas are similar to microwave and radiofrequency (RF) antennas and can couple electromagnetic radiation in the visible and infrared just like other antennas do at their corresponding wavelengths [5]. Although similar, there are crucial differences between optical antennas and their microwave and RF counterparts due to their nano size and the resonant properties of metal nanostructures [8].

A. Theory of Operation

Electromagnetic waves induce time-varying electric fields in metals that exert a force on the gas of electrons inside the material, causing the charge carriers to oscillate in a collective movement [9]. This phenomenon is known as surface plasmon and it constitutes the basis for the optical phenomena that gives rise to the unique optical properties associated with nanoantennas, which are extremely valuable for the harvesting and absorption of solar energy. The theory behind this phenomenon will be adressed in more detail in III.A.1).

If the resonant frequency of the designed nanoantenna matches the incoming wavelength frequency it leads to the absorption of the incoming EM radiation [9]. The efficiency rate of absorption of the incident radiation depends on the design of antenna resonance, and impedance matching of the antenna. Nevertheless, modelling and experimental measures performed in [5] show that nanoantennas can eventually absorb close to 90% of the available in-band energy. Furthermore, nanoantennas can utilize both the visible and IR regions of the light spectrum as well as the reradiated IR energy, capturing the energy of the Sun during the day but also the radiation of the Earth at night.

B. Technical Framework

During recent years, a lot of research has been developed regarding different configurations and properties of nanoantennas for various applications. However, these devices still face some challenges and there is a need for improvements.

Some of the challenges associated to nanoantennas concern the size of all elements, which must be extremely small, and the device must be capable of efficiently capture all polarizations of the incident radiation [10] [12]. To do this successfully without the need for a sun-tracking system means that the acceptance angle must always be as wide as possible. It is also important to consider the impedance and capacitance of the antenna. Furthermore, in order to create an efficient nanoantenna, the choice of materials and design of the device are crucial.

In this study, the analysis will be focused on the implementation of a metallic aperture nanoantenna into a solar cell. More specifically, a metallic subwavelength aperture nanoantenna array. Aperture nanoantennas are able to increase coupling efficiency of nearby light by focusing it onto an aperture region, which enables light confinement and better control of the radiation pattern [13]. Since the practical use of subwavelength apertures to enhance light-matter interaction

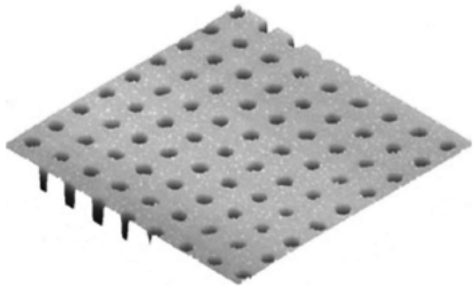

Fig. 1: Subwavelength aperture nanoantenna array (Adapted from [14]).

first took place, the interest in the Extraordinary Optical Transmission (EOT) phenomenon keeps increasing and has already led to much research on the origin of the phenomenon, the influence of several design parameters (aperture shape and dimensions, metal permittivity, metal adhesion layer) and the development of practical applications [14]. Arranging the apertures in a subwavelength array with a periodic pattern, as illustrated in figure 1 can provide extra coupling capabilities. However, there are dependencies regarding hole size, lattice spacing, metal film thickness, and angular dispersion. Several other parameters also have significant importance such as type of metal, symmetry in the dielectric-metal-dielectric layer stack, finite-size effects of the lattice, and the hole shape [15]. The transmission peaks observed in the far-field and the intensity enhancement in the near-filed, characteristic of the aperture array, are consequence of two different resonant phenomena: the resonant excitation of surface plasmon waves at the metal-dielectric interface and the localized plasmon modes on properly shaped apertures [14].

III. Theorical Foundations

Classic diffraction theories do not predict the existence of extraordinary optical transmission (EOT), nor the generation and propagation of surface plasmon polaritons (SPPs), that give rise to the unique optical properties that nanoantennas are associated with. Hence, these phenomena cannot be analysed or supported by such theories. Wave propagation theories regarding light-matter interactions can better describe the overall phenomenon.

A. Light-matter Interactions

1) Surface Plasmon

A plasmon is defined as a quantum of a plasma oscillation. In the same way that light consists of photons, plasmon oscillation consists of plasmons. Thus, plasmons are collective oscillations of the electrons in a plasma. These oscillations are traveling waves with a well-defined frequency and wave vector. When such oscillations exist at the interface between a conductor and a dielectric, such as a dielectric-metal interface, they are called surface plasmons (SPs). Plasmon oscillations

can couple the light in the form of a surface wave creating surface plasmon polaritons (SPPs). A polariton is the result of strong coupling between electromagnetic waves and an electric or magnetic dipole [16]. For a dipole structure, such as an array of slits, an aperture or even a corrugation on the surface, where light is incident on, the photons can excite coherent fluctuations of free electron charges at the metal boundary, creating plasmon oscillations. Such oscillations can couple with the incident light creating polaritons that will propagate at the interface [16].

The resonant interaction between the surface charge oscillation and the electromagnetic field of the light gives rise to unique properties. The presence of SPPs helps to concentrate and channel light using subwavelength structures, which leads to an electric field enhancement that can be used to manipulate interactions between light and matter and improve the transmission of light by the structure [18]. However, for polaritons to be created, the metal needs to exhibit an electric permittivity with a negative real part at the frequency of the incident light. Hence gold, silver, platinum, or aluminum are typically the materials of choice since all of them satisfy this condition. Also, the vector component of the incident light parallel to the interface should be matched with the wave number of the SPP [17].

2) Extraordinary Optical Transmission

The first diffraction theory by a single slit with subwavelength dimensions was developed by Bethe and later by Bouwkamp, resulting in the Bethe-Bouwkamp diffraction theory. The theory predicted that the power transmitted through the slit would decrease as the diameter of the slit decreased far below the radiation wavelength. However, these predictions were refuted in 1998 when Ebbesen observed the so-called extraordinary optical transmission (EOT) phenomenon for the first time [17].

Extraordinary optical transmission (EOT) is defined as an optical phenomenon in which a structure, containing subwavelength apertures in an opaque screen, transmits more light than would be expected. In EOT, the nanostructure enables a several orders of magnitude larger transmission efficiency than that predicted by the classical aperture theory [11]. In Ebbesen experiments, this nanostructure was an array of cylindrical holes, with a certain periodicity constant, hole diameter, and thickness. The array displayed sharp peaks in transmission for wavelengths as large as ten times the diameter of the holes. For these wavelengths, the transmission efficiency (normalized to the total area of the holes) could even exceed unity. These unique optical properties are due to plasmons coupling with light on the surface of the metal film thus creating polaritons (SPPs) [19]. The EOT phenomenon offers the possibility of a variety of applications due to the high transmission efficiencies and the high local field enhancements that can be achieved [15].

IV. Model Structure and Configuration

To study the problem submitted in this investigation, 2D and 3D models of different solar cells structures are simulated. All the simulations are developed using *COMSOL Multiphysics*®. The software allows simulation of physics-based systems described by partial differential equations (PDEs). However, in most of the problems these equations cannot be solved by analytical methods. Thus, the Finite Element Method (FEM) is used to compute the approximation of the actual solution of the PDE.

All the simulations are performed using the *Electromagnetic Waves, Frequency Domain* module of the software, which uses FEM to solve the frequency domain form of Maxwell´s equations. For this interface, the dependent variable is the total electrical field and the governing equation being solved for is given by [21]:

$$\nabla \times (\mu_r^{-1} \nabla \times \mathbf{E}) - k_0^2 \times \epsilon_{rc} \times \mathbf{E} = 0 \tag{1}$$

where μ_r is the relative permeability, ϵ_{rc} is the relative permittivity, k_0 is the wave number, and $\mathbf{E}$ is the electric field. In 2D models, the electric field varies with the out-of-plane wave number k_z as presented in (2) [21].

$$\mathbf{E}(x, y, z) = \widetilde{\mathbf{E}}(x, y) e^{-ik_z z} \tag{2}$$

The *Electromagnetic Waves, Frequency Domain* physics interface is an optical module thus it is necessary to characterize the optical constants *n* and *k* of each material of the simulated structure, where *n* is the refractive index and *k* the extinction coefficient. The models used for each material are retrieved from an online database [22], which presents the same models as the ones available on *COMSOL Multiphysics*®.

A. 2D Model

The geometry of the simulated 2D model is represented in figure 2a and is constituted by an amorphous silicon (a-Si) cell and by a dielectric layer on top, which in this case is air. Although a typical solar cell has n-type and p-type layers, the three layers represented in the nanostructure are all composed of intrinsic amorphous silicon. The absorption of light in a solar cell occurs mainly in the intrinsic region of the cell hence, it can be assumed that the n-type and p-type doped layers do not contribute in a significant manner to the generation of photocurrent in the solar cell [20]. Therefore, for the purpose of simplifying the following simulations, the nanostructure illustrated in figure 2 is considered as an actual a-Si PIN solar cell. An aluminium (Al) nanoantenna with apertures was later introduced on top of the silicon cell, as illustrated in 2b, to study the differences in the optical response of the cell with and without a nanoantenna.

In both versions of the 2D model, the incident electric field, defined by $|E_0| = 1\mu$V/m, is generated on top of the structure. The electric field amplitude should be parallel to the nanoantenna array in order to reach the nanoantenna's apertures in a tangential manner. For a metal nanoantenna in the visible and near-infrared regions, the EM field wave vector must have a parallel component to the surface of the metal in order for polaritons to be originated and therefore, for the EOT phenomenon to take place [16]. Hence, the incident

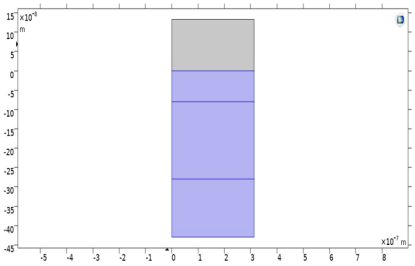

(a) Schematic representation of the simulated 2D structure without nanoantenna.

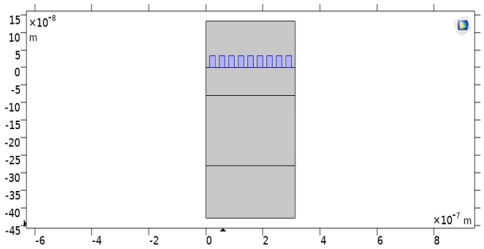

(b) Schematic representation of the simulated 2D structure with nanoantenna.

Fig. 2: Schematic representation of the simulated 2D a-Si solar cell model.

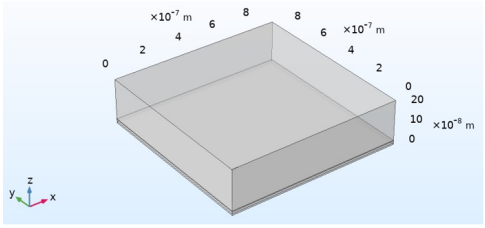

(a) Schematic representation of the simulated 3D a-Si solar cell structure without nanoantenna.

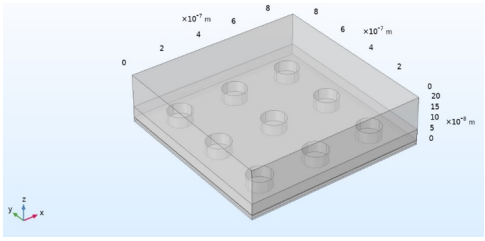

(b) Schematic representation of the simulated 3D a-Si solar cell structure with nanoantenna.

Fig. 3: Schematic representation of the simulated 3D a-Si solar cell model.

electric field amplitude is defined in the x axis direction, as $|E_x| = |E_0|$ V/m and $|E_y| = |E_z| = 0$ V/m. The EM field amplitude will vary in the x direction, but the EM field wave will propagate in the y axis direction.

B. 3D Model

To further deepen the study of a nanoantenna coupled to a solar cell it is important to analyse the performance of 3D models. The environment and conditions defined in a 3D model resemble actual reality in a more truthful way, so the optical response given by the cell and the occurrence of EOT can be examined in a more detailed and accurate manner.

1) Amorphous Silicon (a-Si) Solar Cell Structure

Similarly to what was established in 2D, two versions of the 3D model are created: without and with a nanoantenna, as represented in figures 3a and 3b, respectively. The materials of the 3D model are the same as those implemented in the 2D model. An electric field, defined by $|E_0| = 1\mu$V/m, is generated on the top external boundary of the dielectric layer in the 3D structure. The EM field is perpendicular to the nanoantenna, having the opposite direction of the z axis, and it is defined in the generation port by $|E_x| = |E_y| = \frac{E_0}{\sqrt{2}}$ V/m and $|E_z| = 0$ V/m. All the remaining simulation requirements and specifications are equivalent in both 2D and 3D models, with or without the nanoantenna.

2) PIN Solar Cell Structure

As previously mentioned, the solar cell implemented in the structures described in IV.A and IV.B.1) is composed of only intrinsic amorphous silicon, since it is presumed that the n- and p-doped regions of solar cells do not significantly contribute to the production of photocurrent. Nevertheless, in an attempt

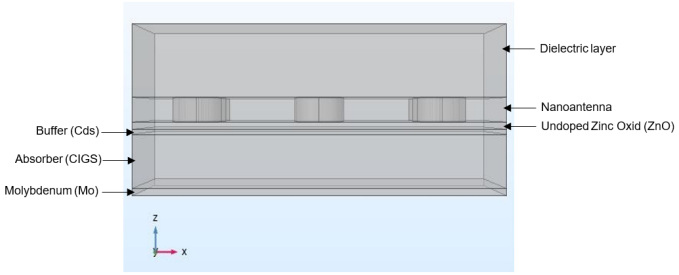

Fig. 4: Side view of the simulated 3D CIGS solar cell structure.

to substantiate this assumption an a-Si PIN solar cell structure is developed and posteriorly simulated, to ultimatly compare the results with the original model (described in IV.B.1). The model in question has the exact same geometry and dimensions as the original 3D a-Si solar cell structure characterized in IV.B.1). The simulation specifications are also equivalent to the ones defined for the original 3D a-Si solar cell structure and the electric field will be generated under the exact same conditions, already depicted in subchapter IV.B.1).

3) CIGS Solar Cell Structure

The study and assessment of the output optical response of a 3D model using a different type of solar cell would be noteworthy. Therefore, based on the original 3D model characterized in subchapter IV.B.1), a 3D model with a CIGS solar cell structure is developed, as exemplified in figure 4. The specifications and conditions that were imposed on this model and corresponding simulation are the same as those defined for the models depicted in IV.B.1) and IV.B.2).

V. Simulation Results

The simulations that follow are accomplished using four different boundary probes, one at the end of each layer of the structure. Those probes analyse the maximum ratio between the electric field norm and the incident electric field norm, $|\frac{E}{E_0}|$. If the simulated structure has the ability to transmit more light than its incidence, then the value obtained for the ratio is equal or greater than 1, indicating the occurrence of Extraordinary Optical Transmission.

A. 2D Simulations

As seen in figure 5a, regarding the optical response of the 2D model without nanoantenna, the maximum ratio does not reach values above or even equal to 1, meaning that the EOT phenomenon did not take place. However, this result is to be expected since without the presence of any subwavelength aperture, SPP's will not be generated, and extraordinary transmission cannot happen. It is important to underline that SPP's constitute the main agents of EOT in metallic nanoantennas, functioning in the visible and near-infrared region of the light spectrum. Finally, since the amplification of the electric field is not verified in any of the layers of the structure, the electric field will simply decay along the propagation distance.

On the other hand, when analysing figure 5b, it is possible to determine that the EOT phenomenon did in fact occur, since values of $|\frac{E}{E_0}|$ greater than 1 were obtained for boundary probe 1. Naturally, this will be the boundary that presents the best results since it is located directly underneath the nanoantenna array, which is where surface plasmon polaritons are going to be generated and propagate. However, the EOT phenomenon occurrence did not influence the results of the remaining boundary probes. In fact, the values obtained by these probes are quite similar to those obtained by the model without the nanoantenna. In order for the results of those probes, that regard the second and third layer of the a-Si cell, to be almost unaltered, the majority of the absorption had to have occurred in the first layer of the cell, where boundary probe 1 is located.

It is important to stress that the results obtained for the boundary probes located within the a-Si solar cell represent the electric field that was not absorbed by the cell being that, at the output of the cell, this value should be as low as possible. It is crucial to establish that, the greater the difference between the input electric field in the cell or in a certain layer and its output electric field, the greater the absorption. Thus, one can presume that the greater the gap between the normalized electric field values from one probe to the next, the greater the absorption that occurred in that specific layer of the cell, bounded by those probes. Plus, evidently, the more photons are absorbed by the cell, the more electric power can be generated.

Based on the aforementioned premise, figure 6 illustrates the absorption occurring in each layer of the cell. For each layer of the cell, the difference between the intensity values of the output probe and the input probe is computed. Thus, for layers where absorption occurs these values will be negative.

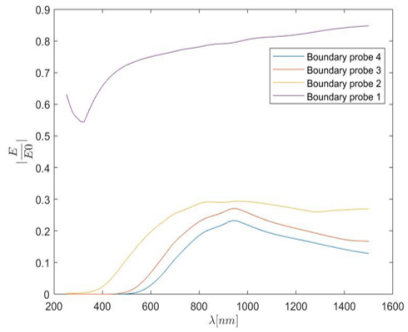

(a) Optical response of the simulated 2D a-Si solar cell structure without nanoantenna.

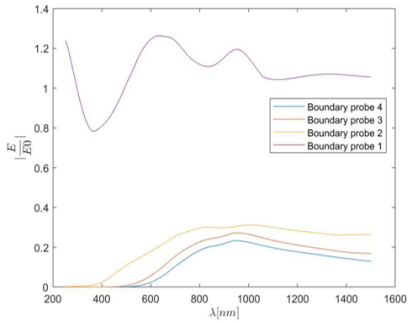

(b) Optical response of the simulated 2D a-Si solar cell structure with nanoantenna.

Fig. 5: Optical response of the simulated 2D a-Si solar cell structures.

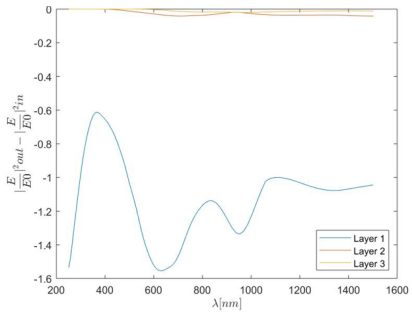

Fig. 6: Absorption curves of the simulated 2D a-Si solar cell structure with nanoantenna.

Therefore, according to figure 6, photons are going to be absorbed essentially in the first layer of the cell (Layer 1), particularly for the incident wavelength regions where field amplification is verified in figure 5b, such as 600 nm and 1000 nm. These results corroborate the conclusions drawn by the analysis of figure 5b.

Finally, taking into account the fact that, due to field amplification, the introduction of the nanoantenna implies that more electrons are available in the first layer of the cell and that the majority of the absorption takes place in this layer, then more electrons are going to be absorbed, resulting in greater generation of electric current.

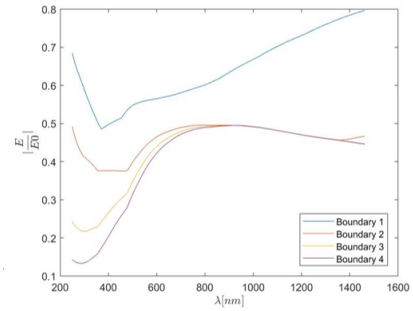

(a) Optical response of the simulated 3D a-Si solar cell structure without nanoantenna.

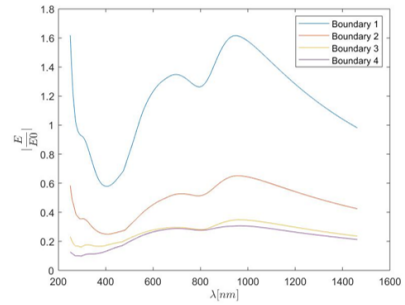

(b) Optical response of the simulated 3D a-Si solar cell structure with nanoantenna.

Fig. 7: Optical response of the simulated 3D a-Si solar cell structures.

B. 3D Simulations

The procedures and conditions applied to carry out the simulation of all the 3D models, with and without the nanoantenna, are identical to those imposed on the 2D model simulations.

1) Amorphous Silicon (a-Si) Solar Cell Structure

As expected, for the amorphous silicon solar cell model without the nanoantenna (figure 3a), the simulation results in figure 7a show that EOT does not occur. Similarly to what was already observed in the 2D models, due to losses endured throughout the air layer and the absorption endured throughout the a-Si cell, the electric field decays along the structure. On the other hand, the results in figure 7b clearly show the presence of EOT, though only for boundary probe 1 located below the nanoantenna array, at the beginning of the solar cell, possibly due to the reduced propagation distance of the SPP's (around nm). This boundary also shows two identifiable peaks in the normalized electric field values, which were not present in the optical response of the model without the nanoantenna. These peaks are obtained for the incident wavelengths of 700 nm and 1000 nm, located in the visible and near-infrared regions, respectively. However, the extraordinary transmission verified in boundary probe 1 did not affect the remaining boundary probes, as the obtained electric field ratio values are quite small, never reaching unitary values.

Figure 8 shows the comparison between the results obtained by each boundary probe in the simulated 3D structure with

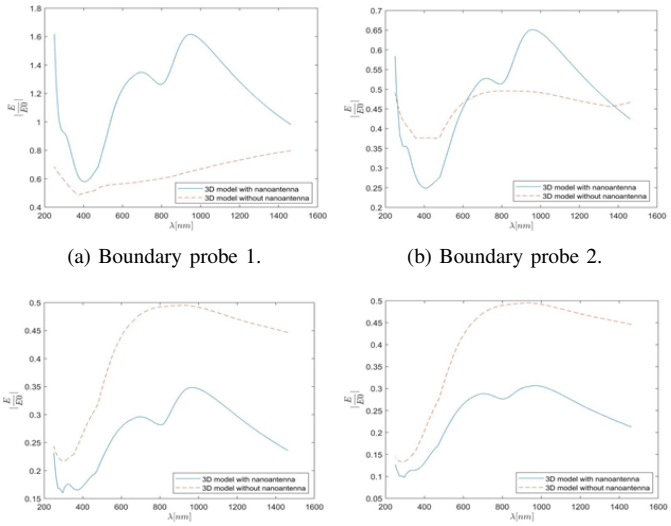

(a) Boundary probe 1. (b) Boundary probe 2.

(c) Boundary probe 3. (d) Boundary probe 4.

Fig. 8: Optical response of the 3D a-Si solar structure with and without nanoantenna.

and without the nanoantenna. Figure 8a, regarding boundary probe 1, can clearly demonstrate the substantial difference in the electric field values when using a model with or without the implementation of a nanoantenna. EOT is present throughout almost the entire incident wavelength range, meaning that the conditions required for the generation of surface plasmon polaritons are met for different regions of the incident light spectrum such as the visible and the infrared region. On the other hand, figure 8b shows that, although EOT is not verified in boundary probe 2, field amplification still exists as can be seen for the incident wavelength interval between 600 nm and 1400 nm. As for figures 8c and 8d, these demonstrate that, in the model with the nanoantenna, the electric field absorption all through the cell is greater since the normalized electric field values obtained for boundary probes 3 and 4 are much smaller than those obtained by the model without the nanoantenna.

This conclusion is supported by figures 9a and 9b, where absorption curves for both scenarios (with and without nanoantenna) are illustrated. By analysing those figures it becomes clear that, for the model with the nanoantenna, the absorption of photons is greater. The increase in absorption is visible in all layers of the cell but specially accentuated in cell's first layer (layer 1), where EOT occurs. Moreover, peaks in absorption correspond to peaks in field amplification observed in figure 7b, for incident wavelengths of 700 nm and 1000 nm. Once again, it is important to stress that greater absorption ultimately results in greater amount of electric power supplied by the cell.

2) Amorphous Silicon (a-Si) Solar Cell Structure: introduction of nanoantenna within the solar cell

The position of the nanoantenna in the nanostructure may be an important factor when it comes to the optical response produced by the model. Hence, a study regarding the introduction of the nanoantenna within the solar cell, between the a-Si

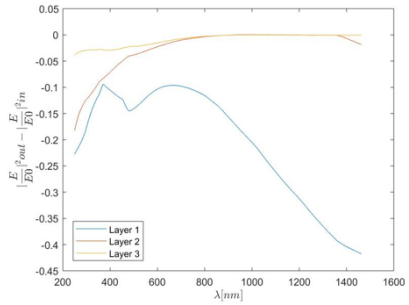

(a) Absorption curves for the simulated 3D a-Si solar cell structure without nanoantenna.

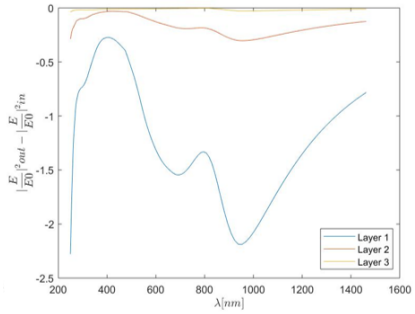

(b) Absorption curves for the simulated 3D a-Si solar cell structure with nanoantenna.

Fig. 9: Absorption curves for the simulated 3D a-Si solar cell structures.

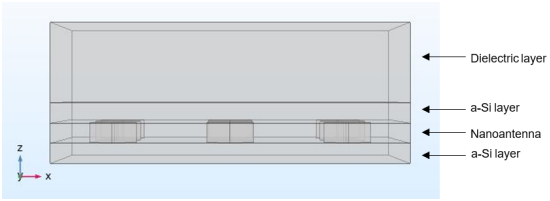

Fig. 10: Side view of the 3D a-Si solar cell structure with nanoantenna within the solar cell.

layers, is carried out. It is noteworthy that for the nanoantenna to be positioned between the layers of the solar cell, the dimensions of the cell had to be modified which means that the optical responses of the models in V.B.1) and V.B.2) cannot be directly compared. The model in question is represented in figure 10.

According to figure 11, extraordinary transmission can be identified for boundary probes 1, 2 and 3. Although the nanoantenna is located between probes 2 and 3, probe 1 is also influenced by the EOT phenomenon that occurs in the nanoantenna. Nevertheless, the presence of EOT or any field amplification is confined to the infrared region, as demonstrated by the distinguishable peaks produced by all boundaries in that exact region of the wavelength spectrum. Due to the location of the nanoantenna, the incident light reaches the device having already propagated trough one layer of a-Si (the cell's first layer), meaning that absorption of

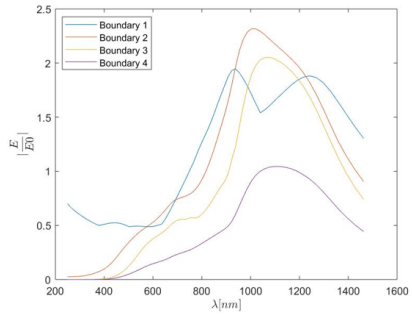

Fig. 11: Optical response of the simulated 3D a-Si solar cell structure with nanoantenna within the solar cell.

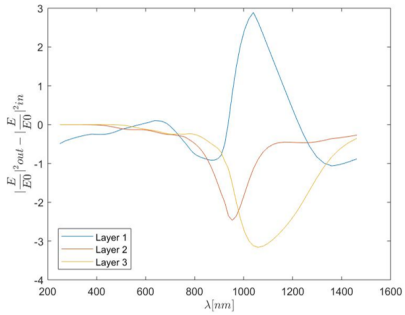

Fig. 12: Absoption curves of the simulated 3D a-Si solar cell structure with nanoantenna within the solar cell.

photons with energy levels equal or higher than the energy gap level (for wavelengths equal or lower) of a-Si which is 1.6 eV corresponding to 775 nm, has already occurred. This ultimately implies that the radiation influenced by the nanoantenna will be mainly located in incident wavelengths after the 775 nm mark, regarding the infrared region. Figure 12 corroborates this reason, since absorption is verified within the cell's first layer (layer 1) until the 600 nm mark, followed by a substantial increase in absorption for the second and last layers of the cell (layer 2 and layer 3), already in the infrared region of the spectrum which is also the region that presented greater field amplification.

3) Amorphous Silicon (a-Si) Solar Cell Structure: introduction of nanoantenna with conical holes

The geometry of the holes in the nanoantenna is also an important element to take in consideration when analysing the output optical response of the model. Therefore, to study the influence of this factor, conical holes are implemented in the nanoantenna layer of the original structure, resulting in the 3D structure illustrated in figure 13. The conical geometry of the nanoantenna holes could perhaps result in improved concentration of the incident radiation which could lead to greater field amplification.

Figure 14 makes the comparison between the optical response of the a-Si solar cell structure with the nanoantenna with cylindrical holes and with conical holes. Since the geometry of the nanoantenna holes may eventually influence

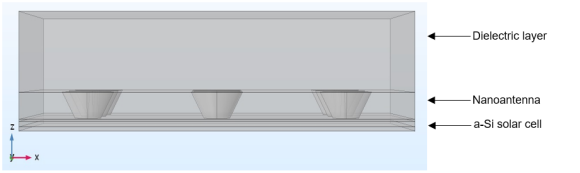

Fig. 13: Side view of the 3D a-Si solar cell structure with nanoantenna with conical holes.

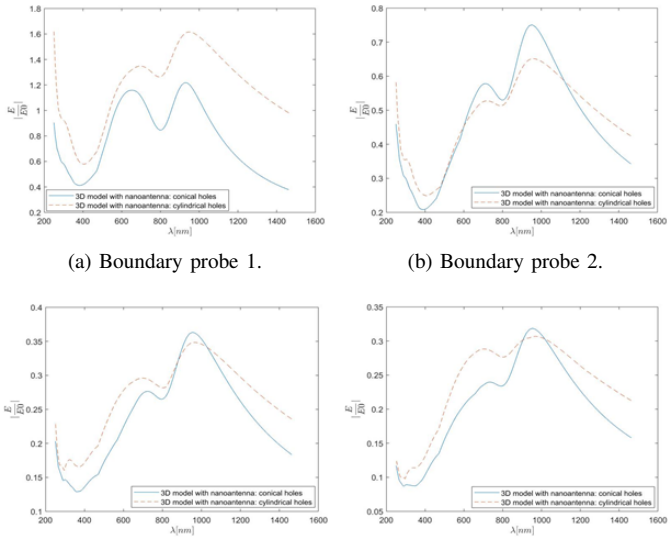

(a) Boundary probe 1.

(b) Boundary probe 2.

(c) Boundary probe 3.

(d) Boundary probe 4.

Fig. 14: Optical response of the simulated 3D a-Si solar cell structure with nanoantenna with conical holes versus nanoantenna with cylindrical holes.

the occurrence of EOT, the results in boundary probe 1 are particularly relevant since this boundary is located directly underneath the nanoantenna, where EOT takes place. However, according to figure 14a, the use of conical holes, instead of cylindrical holes, does not result in greater extraordinary transmission since, for the model with cylindrical holes, results clearly show greater field amplification in boundary probe 1. Regarding the remaining boundary probes, the output optical spectra produced by both models, although not equal, show no significant differences.

4) Amorphous Silicon (a-Si) PIN Solar Cell Structure

The comparison between the output optical response of the a-Si PIN solar cell structure without nanoantenna, and the output optical response of the a-Si solar cell structure also without nanoantenna is illustrated in figure 15a. It is possible to verify that the generated spectra of both models are extremely similar, since these overlap along the entire incident wavelength range, with the exception of the minor divergence that occurs at the end of that range, around 1400 nm.

A similar situation can be observed in figure 15b, illustrating the comparison between the output optical response of the a-Si PIN solar cell structure and the output optical response of the a-Si solar cell structure, both with nanoantenna. Although

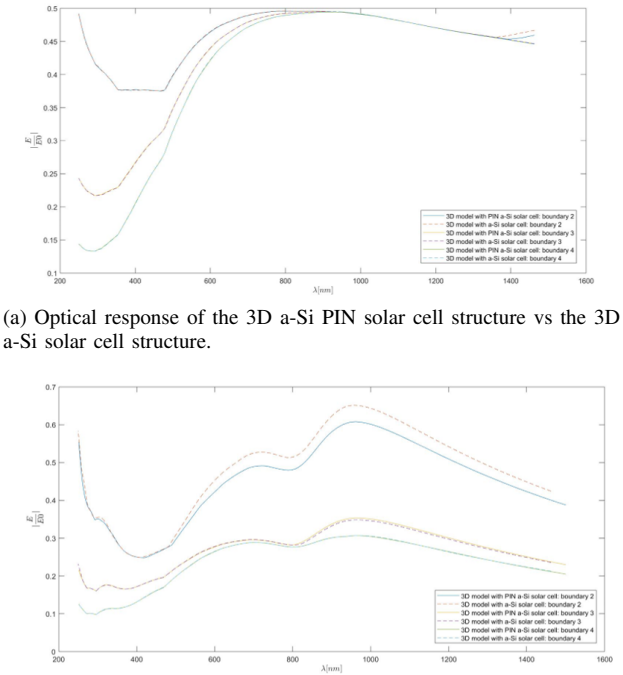

(a) Optical response of the 3D a-Si PIN solar cell structure vs the 3D a-Si solar cell structure.

(b) Optical response of the 3D a-Si PIN solar cell structure with nanoantenna vs the 3D a-Si solar cell structure with nanoantenna.

Fig. 15: Optical response of the simulated 3D a-Si PIN solar cell strcuture vs the 3D a-Si solar cell structure.

in this case the results obtained by boundary probes 2 and 3 slightly vary between the two models, this difference can be considered negligible.

Overall, the results obtained by the simulations using both models, with and without nanoantenna, are quite similar. Therefore, although the optical responses of the two models are not exactly equal, they validate the decision to consider the structure composed of intrinsic a-Si as an actual a-Si PIN solar cell in order to simplify the performed simulations.

5) CIGS Solar Cell Structure

The procedures necessary to simulate the CIGS solar cell model are identical to those defined in all previous simulations. Nevertheless, these following simulations measure the maximum absolute values of the normalized electric field using five, instead of four, different boundary probes located at the end of each layer of the structure. This is obviously due to the fact that the CIGS solar cell defined in this structure has one more layer than the a-Si solar cell used in the other models.

By examining figure 16a, it is possible to observe that, for the first three boundary probes, the normalized electric field reaches values equal to 1 or higher even without the presence of a nanoantenna, especially in the infrared region of the spectrum. This gain is typically associated to the material of the structure in question, which in this case corresponds to the materials present in the first two layers of the CIGS solar cell: ZnO and Cds. If the dielectric function of a certain material has an imaginary part greater than zero then it would be possible to find electric field amplification within that material, possibly

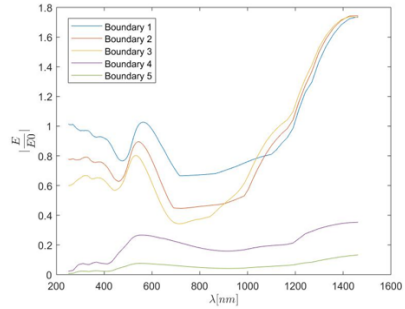

(a) Optical response of the 3D CIGS solar cell structure without nanoantenna.

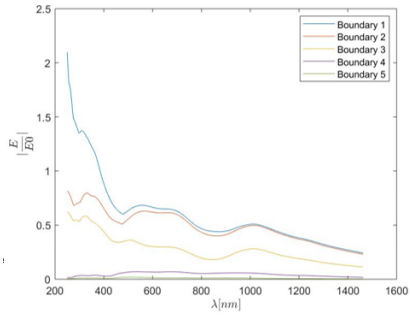

(b) Optical response of the 3D CIGS solar cell structure with nanoantenna.

Fig. 16: Optical response of the simulated 3D CIGS solar cell structure.

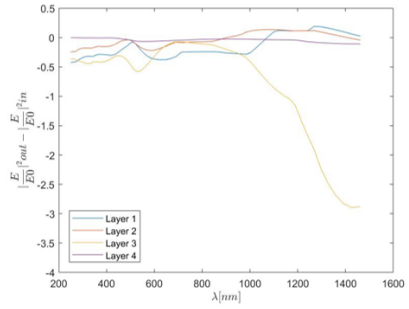

(a) Absorption curves of the 3D CIGS solar cell structure without nanoantenna.

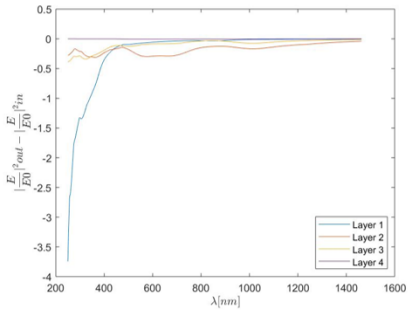

(b) Absorption curves of the 3D CIGS solar cell structure with nanoantenna.

Fig. 17: Absorption curves of the simulated 3D CIGS solar cell structure.

obtaining values bigger than 1 for the normalized electric field, even without the presence of any type of subwavelength aperture. However, it is important to note that almost no absorption occurs throughout these first two layers of the cell, as verified in figure 17a. In fact, the results in this figure also show that the third layer of the cell (layer 3), the CIGS layer, is the only layer where absorption occurs in a significant manner. The absorption is focused on the infrared region since CIGS cells typically absorb radiation consistent with that exact region of the spectrum, as their energy band gap can be tuned roughly from 1.01eV to 1.68eV corresponding approximately to 1230nm and 740nm, respectively.

When the implementation of the nanoantenna occurs on top of the CIGS solar cell, the obtained optical response, represented in figure 16b, is quite underwhelming when it comes to the observation of the EOT phenomenon. The values obtained for the normalized electric field are quite low in the first boundary probes if compared to those obtained without the nanoantenna. However, in boundary probe 1, a peak in the normalized electric field can be observed around the 250 nm mark, in the UV zone of the light spectrum, and EOT is present until 400 nm. Also, although the simulation wavelength range starts at 250 nm, the results suggest that perhaps greater field amplification occurs for even smaller incident wavelengths, since the normalized electric field values seem to be decreasing along the wavelength spectrum. According to figure 17b, the absorption of photons in the CIGS layer (layer 3) is significantly inferior in this scenario when compared to the model without the nanoantenna. Nevertheless, absorption did increase in the second layer of the cell (Cds layer) and specially in the first layer of the cell (ZnO layer). Plus, most of the absorption of photons throughout all layers now concerns photons in the UV region of the light spectrum.

VI. Conclusion

The main goal of this investigation is to study the behaviour of a solar cell with the integration of an optical nanoantenna. The coupling of nanoantennas to solar cells could eventually constitute a breakthrough regarding solar energy harvesting on PV panels, due to the concentration and amplification of solar irradiance, resulting in more incident energy and, therefore, more generation of output power.

The 2D and 3D simulations of different solar cell structures, with and without a nanoantenna, allow to observe and assess how the optical response of such structures is influenced by the presence of the nanoantenna, and if extraordinary optical transmission (EOT) occurs.

Based on 2D and 3D results regarding the a-Si solar cell structure, simulated from V.A. to V.B.1), it can be confirmed that EOT does always occur when an aluminum nanoantenna is coupled to the solar cell structure, which ultimately implies that these structures were able to transmit more light than its

incidence. Additionally, an increase in absorption is noticeable when the nanoantenna is coupled to the cell, especially in the first layer (between boundary probe 1 and boundary probe 2). These results are quite promising since the more photons are absorbed by the cell, the more electron-hole pairs are generated by the photovoltaic effect, and more electric power will be made available by the cell, for a certain operation point. It is also noteworthy that in both 2D and 3D simulation scenarios, the obtained optical responses for the models with nanoantennas, showed peak normalized electric field values for incident wavelengths in the visible and infrared regions. These findings indicate that the implementation of nanoantennas in solar cells can be pertinent for applications using different parts of the light spectrum.

Furthermore, results in V.B.2) suggest that the position of the nanoantenna in the structure can affect the light spectrum region where EOT takes place, since the observed extraordinary transmission and field amplification were limited to the infrared section of the incident wavelength range. This trait might prove to be useful for certain applications functioning at night or in places with little sunlight, since infrared radiation is still present.

Regarding the impact that the shape of the holes in the nanoantenna array can have in the optical response of the structure, results obtained in V.B.3) show that the 3D model with nanoantenna with conical holes produced similar output spectra to those obtained by the 3D model with nanoantenna with cylindrical holes. Except when it came to the normalized electric field values, mainly in boundary probe 1 located directly below the nanoantenna, for which the model with cylindrical holes did present, for the entire wavelength range, higher electric field values. This signals to the fact that EOT is more accentuated in this type of model, therefore leading to the conclusion that the conical holes geometry is perhaps unsuitable.

Finally, simulations regarding the CIGS solar cell structure illustrated underwhelming results regarding the occurrence of EOT in this particular model, where evidence of extraordinary transmission was only found in boundary probe 1 for a very small range of incident wavelength. Nevertheless, the field amplification that did occur was focused in the UV region of the light spectrum, which can prove useful for certain applications within that range of incident wavelength.

Overall, it was demonstrated that extraordinary optical transmission (EOT) does occur when a nanoantenna is coupled with a solar cell and, more importantly, that the structure produces promising results regarding field amplification and increase in absorption of photons throughout the solar cell. In this study the focus is on the integration of nanoantennas in solar cells to improve solar energy harvesting and, consequently, increase electric power production. Taking this into account, the original 3D a-Si solar cell structure with nanoantenna, characterised in IV.B.1), illustrated in figure 3b, and simulated in V.B.1), is the most suitable and optimized option for this specific purpose since it presented field amplification along the entire incident wavelength spectrum and greater absorption of photons mainly in the first layer of the cell. Nevertheless, the remaining models that were studied presented slight variations that might prove useful under different conditions or for other applications.

References

[1] U.E.I. Administration, "International Energy Outlook 2019", 2019.

[2] R. Castro, "Uma Introdução Às Energias Renováveis: Eólica, Fotovoltaica e Mini-hídrica", 2nd ed., IST- Instituto Superior Técnico, p. 309, 2012.

[3] D. K. Kotter, S. D. Novack, W. D. Slafer and P. Pinhero, "SOLAR NANTENNA ELECTROMAGNETIC COLLECTORS", in *Proceedings of the 2nd International Conference on Energy Sustainability*, Jacksonville, Florida, USA, 2008.

[4] A. M. Sabaawi, C. C. Tsimenidis and B. S. Sharif, "Analysis and Modeling of Infrared Solar Rectennas", *IEEE Journal on Selected Topics in Quantum Electronics*, vol. 19, no. 3, 2013.

[5] D. K. Kotter, S. D. Novack, W. D. Slafer and . P. J. Pinhero, "Theory and manufacturing processes of solar nanoantenna electromagnetic collectors", *Journal of Solar Energy Engineering, Transactions of the ASME*, vol. 132, no. 1, pp. 141-149, 2010.

[6] B. Berland, "Photovoltaic Technologies Beyond the Horizon: Optical Rectenna Solar Cell", Littleton, Colorado, 2001.

[7] L. Novotny and N. F. Van Hulst, "Antennas for light", *Nature Photonics*, vol. 5, no. 2, pp. 83-90, 2011.

[8] National Academy of Engineering, Frontiers of Engineering: Reports on Leading Edge Engineering from the 1999 NAE Symposium on Frontiers of Engineering, 2000.

[9] M. Ameziane, "SOLAR NANOANTENNA ELECTROMAGNETIC", 2015.

[10] L. Mescia and A. Massaro, "New Trends in Energy Harvesting from Earth Long-Wave Infrared Emission", *Advances in Materials Science and Engineering*, 2014.

[11] I. S. Maksymov, "Magneto-plasmonic nanoantennas: Basics and applications", *Reviews in Physics*, vol. 1, pp. 36-51, 2016.

[12] Z. Zhu, S. Joshi, B. Pelz and G. Moddel, "Overview of optical rectennas for solar energy harvesting", *Next Generation (Nano) Photonic and Cell Technologies for Solar Energy Conversion IV*, vol. 8824, p. 88240, 2013.

[13] Q.-H. Park, "Optical antennas and plasmonics", *Contemporary Physics*, pp. 1-20, 2009.

[14] J. Wenger, "Aperture optical antennas",*Optical Antennas*, pp. 369-386, 2014.

[15] F. J. Garcia-Vidal, L. Martin-Moreno, T. W. Ebbesen and L. Kuipers, "Light passing through subwavelength apertures", *Reviews of Modern Physics*, vol. 82, no. 1, pp. 729-787, 2010.

[16] R. A. Lameirinhas, J. P. N. Torres and A. Baptista, "Sensors Based on Nanoantennas: Fundamentals",*European Journal of Applied Physics*, vol. 2, no. 3, 2020.

[17] R. D. F. R. Gomes, M. J. Martins, . A. Baptista and J. P. N. Torres, "Study of a nano optical antenna for intersatellite communications", *Optical and Quantum Electronics*, vol. 49, no. 4, pp. 1-22, 2017.

[18] W. L. Barnes, A. Dereux and T. W. Ebbesen, "Surface plasmon subwavelength optics", *Nature*, vol. 424, no. 6950, pp. 824-830, 2003.

[19] T. W. Ebbesen, H. J. Lezec, H. F. Ghaemi, T. Thio and . P. A. Wolff, "Extraordinary optical transmission through sub-wavelength hole arrays", *Nature*, vol. 391, no. 6668, pp. 667-669, 1998.

[20] I. Massiot, "Design and fabrication of nanostructures for light-trapping in ultra-thin solar cells," Paris, 2013.

[21] Comsol Multiphysics, "Wave Optics Module User's Guide," 2018.

[22] "RefractiveIndex.INFO: Refractive index database," [Online]. Available: https://refractiveindex.info/. [Accessed September 2020].